The Effect of Structural Dimensionality on Carrier Mobility in Lead-Halide Perovskites

Supporting Information

Noor Titan Putri Hartono,[1] Shijing Sun,[1] María C. Gélvez-Rueda,[2] Polly J. Pierone,[3] Matthew P. Erodici,[3] Jason Yoo,[1] Fengxia Wei,[4] Moungi Bawendi,[1] Ferdinand C. Grozema,[2] Meng-ju Sher,[3] Tonio Buonassisi,[1] and Juan-Pablo Correa-Baena[1]**

Affiliations:

[1]Massachusetts Institute of Technology, 77 Massachusetts Avenue, Cambridge, MA 02139
[2]Delft University of Technology, van der Maasweg 9, 2629 HZ Delft, The Netherlands
[3]Wesleyan University, 265 Church Street, Middletown, CT 06459
[4]Institute of Materials Research and Engineering, A*STAR, 2 Fusionopolis Way, Innovis, Singapore, 138634

Figure S1. The single crystal XRD results for DMAPI (dimethylammonium lead iodide/ D), iPAPI (iso-propylammonium lead iodide/ I), and tBAPI (t-butylammonium lead iodide/ T), in comparison to MAPI (methylammonium lead iodide/ M). Note that for the T, due to crystal growth process, H_2O got incorporated into the single crystal structure as shown in the figure. Thus, the single crystal structure for T is in different phase to the thin-film one shown in supporting information Figure S2.

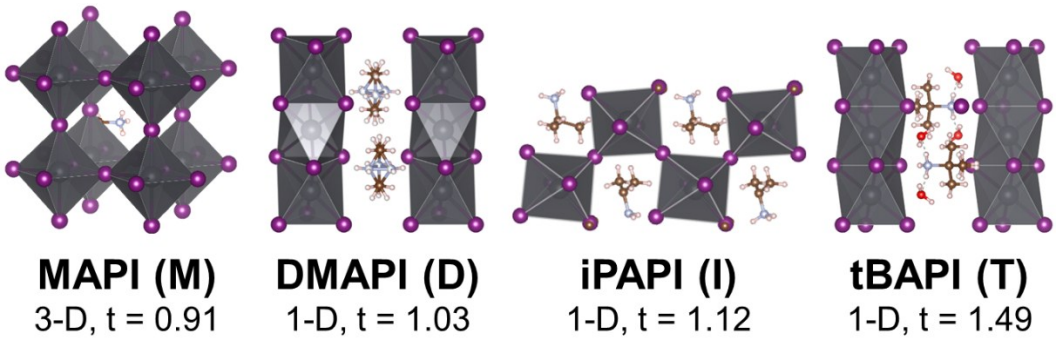

To resolve the previously unknown crystal structure of I and T, single crystals were prepared in order to perform single-crystal XRD. The I single crystal was synthesized using a hydrothermal technique,[1] and the T single crystal was made using a solution cooling technique.[2] The crystal structure of D has been previously resolved by Mancini et al. with a $P6_3/mmc$ space group.[3] The result shows that I has a space group of $P2_12_12_1$ and T has a space group $P2_1/m$, as shown on Figure 1A. Note that the T in single crystal phase is different from the T in thin film phase, since T's single crystal growth in water bath under ambient air introduced water into the structure, which can be observed in supporting information Figure S1. In the bulk, both D and T have a 1D-chain,

edge-sharing structure. I, on the other hand, has a 1D-chain, corner-sharing structure. Interestingly, the increase in size of *A*-site cation does not necessarily correspond to the decrease in structural dimensionality of the bulk material.

Figure S2. The powder XRD results for tBAPI thin film and tBAPI single crystal, indicating they have two different phases.

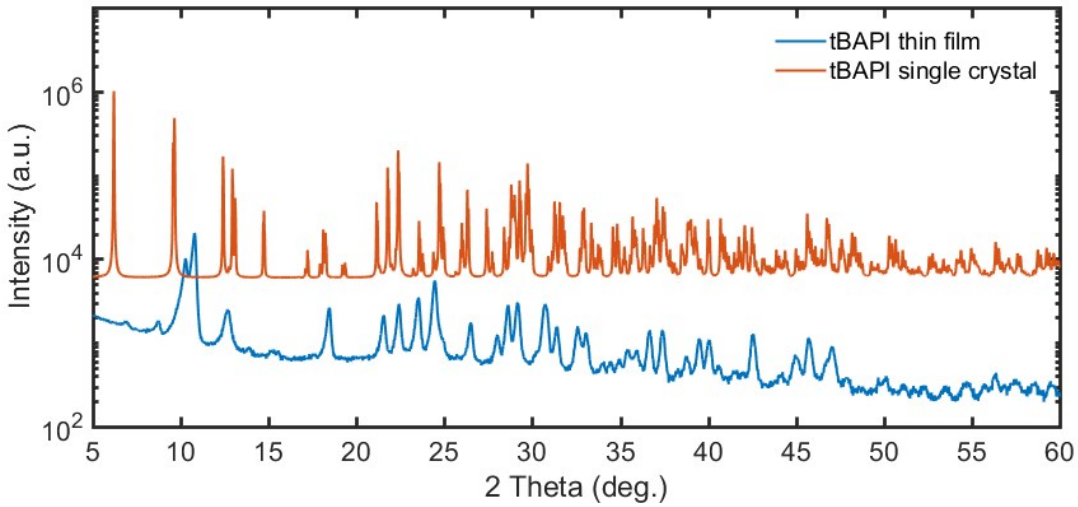

Figure S3. The lattice parameter expansion for **A.** M-D mixtures, and **B.** M-I mixtures.

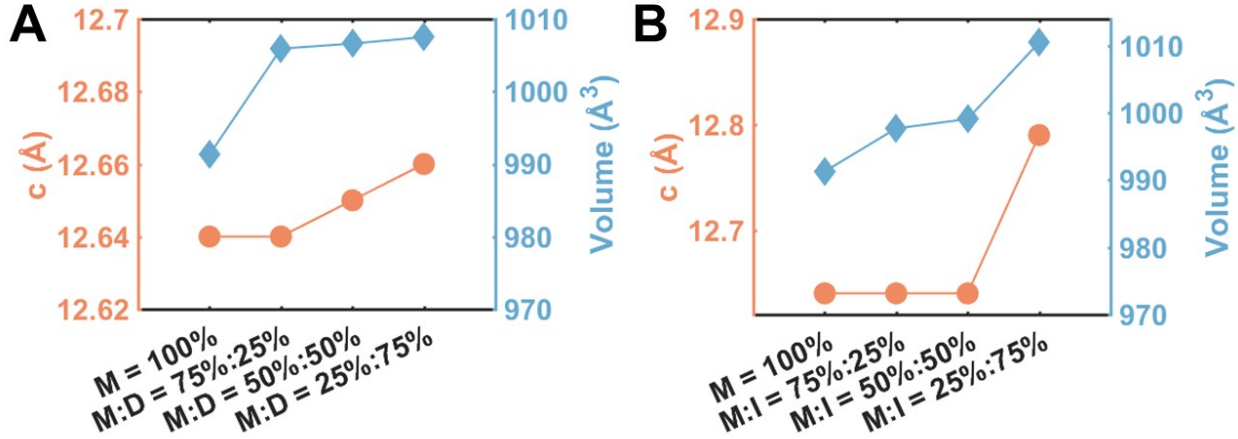

Figure S4. The absorptance of D, I, M, and T.

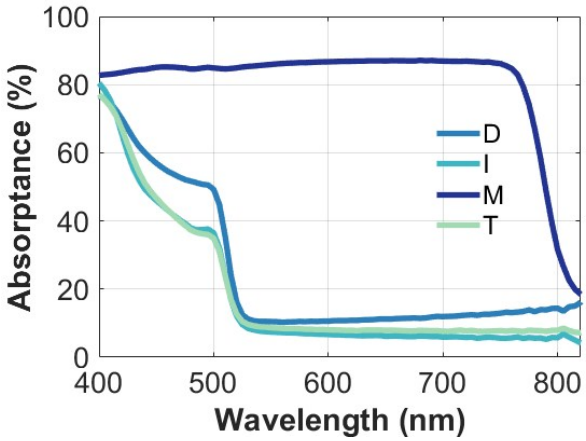

Figure S5. Direct bandgap Tauc plot fitting for both 525 nm and 825 nm absorption onsets for **A.** 100% M, **B.** 75% M: 25% T, **C.** 50% M : 50% T, **D.** 25% M : 75% T, and **E.** 100% T.

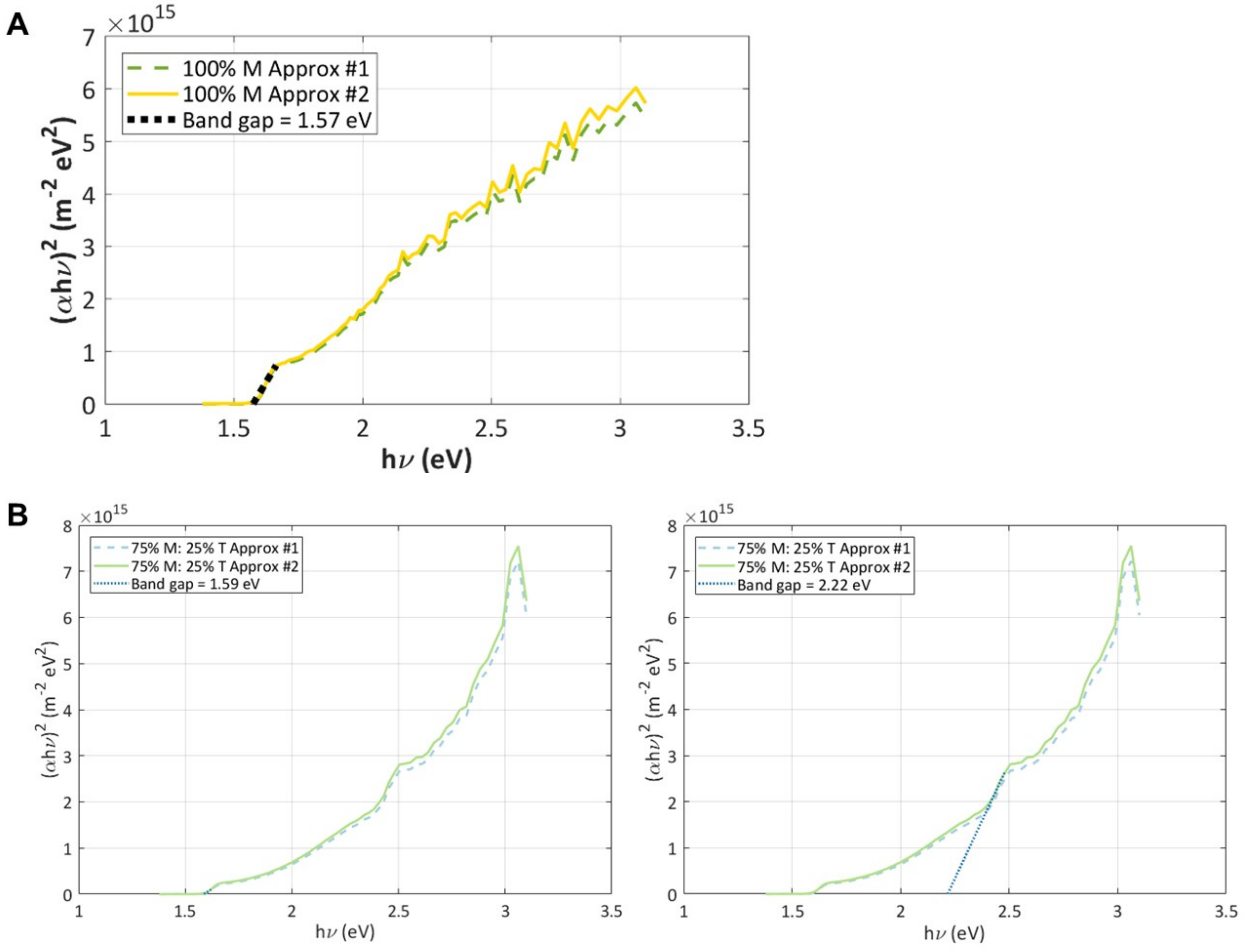

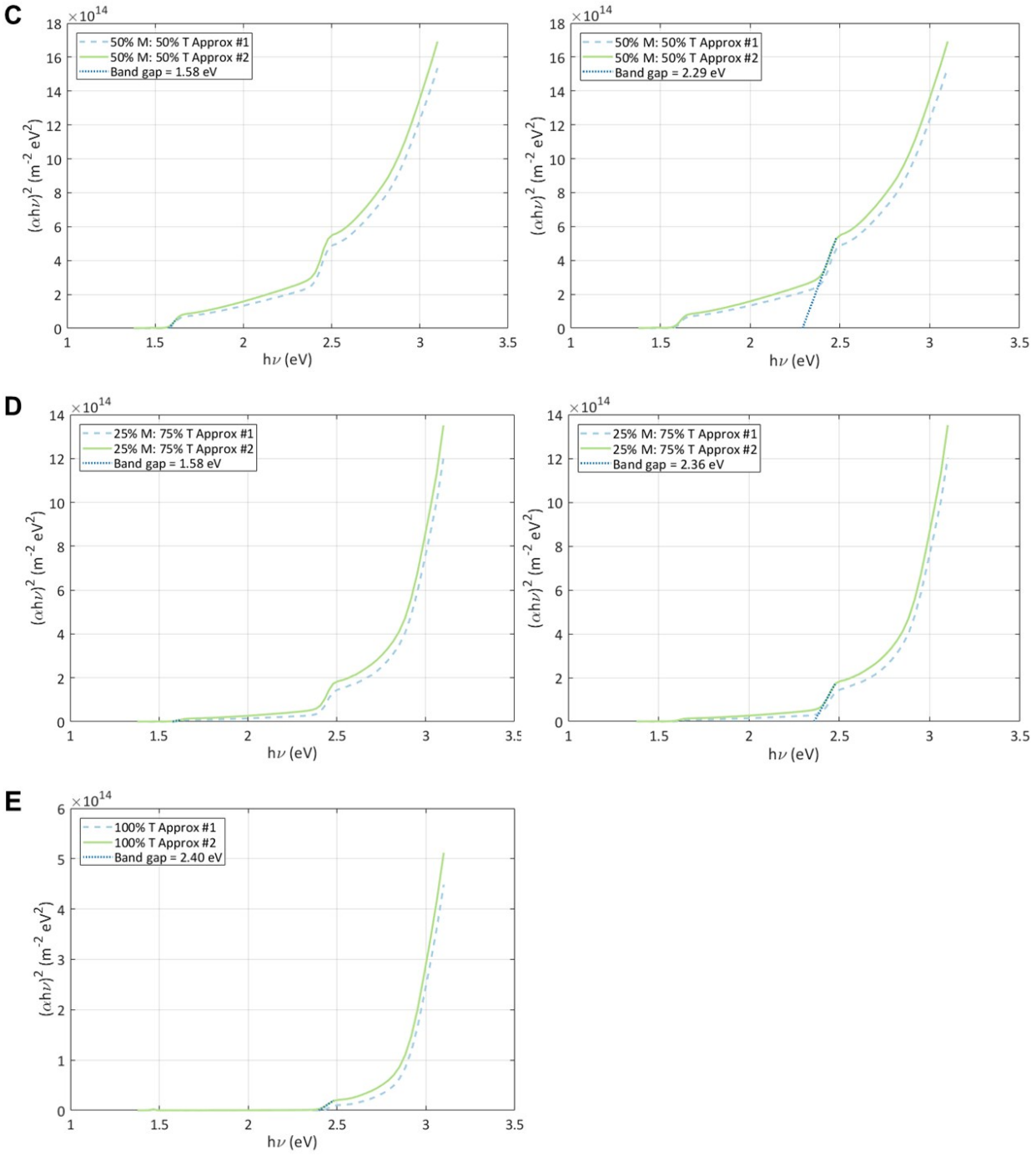

Figure S6. A. The steady-state photoluminescence result for M-T mixtures, excited at 532 nm, which shows a bandgap shift towards higher energy as we add more LD perovskite. **B.** The time-resolved photoluminescence for M-T mixtures. **C.** The corresponding highest lifetime based on biexponential fitting of M-T mixtures PL decay.

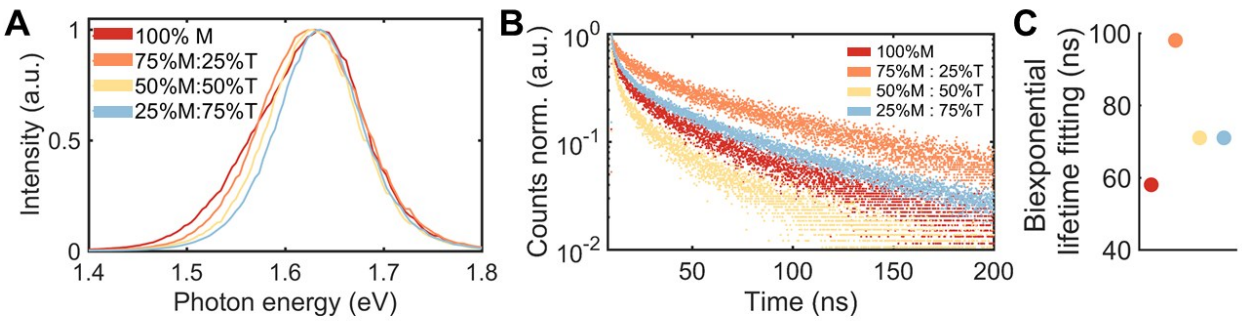

Figure S7. Tauc plot fittings for **A.** direct bandgap from 825 nm absorption onset of 3D/LD mixtures, and **B.** indirect bandgap 3D/LD mixtures.

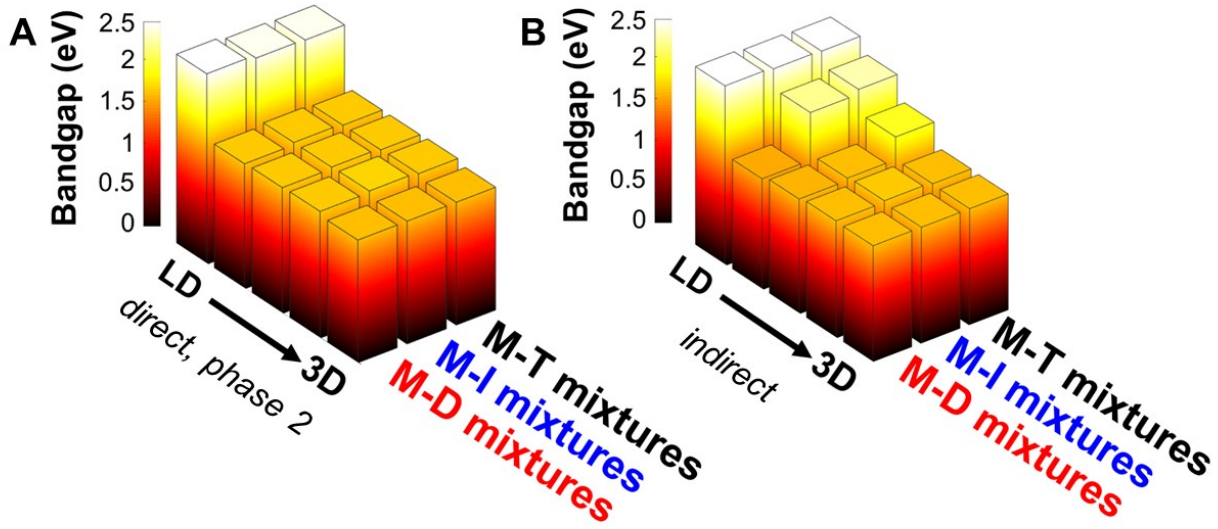

Figure S8. The best device JV curve data for M-D mixtures in reverse (**A.**) and forward (**B.**) direction, M-I mixtures in reverse (**C.**) and forward (**D.**) direction, and M-T mixtures in reverse (**E.**) and forward (**F.**) direction . Each point at JV curve was taken with voltage settling time of 1000 ms.

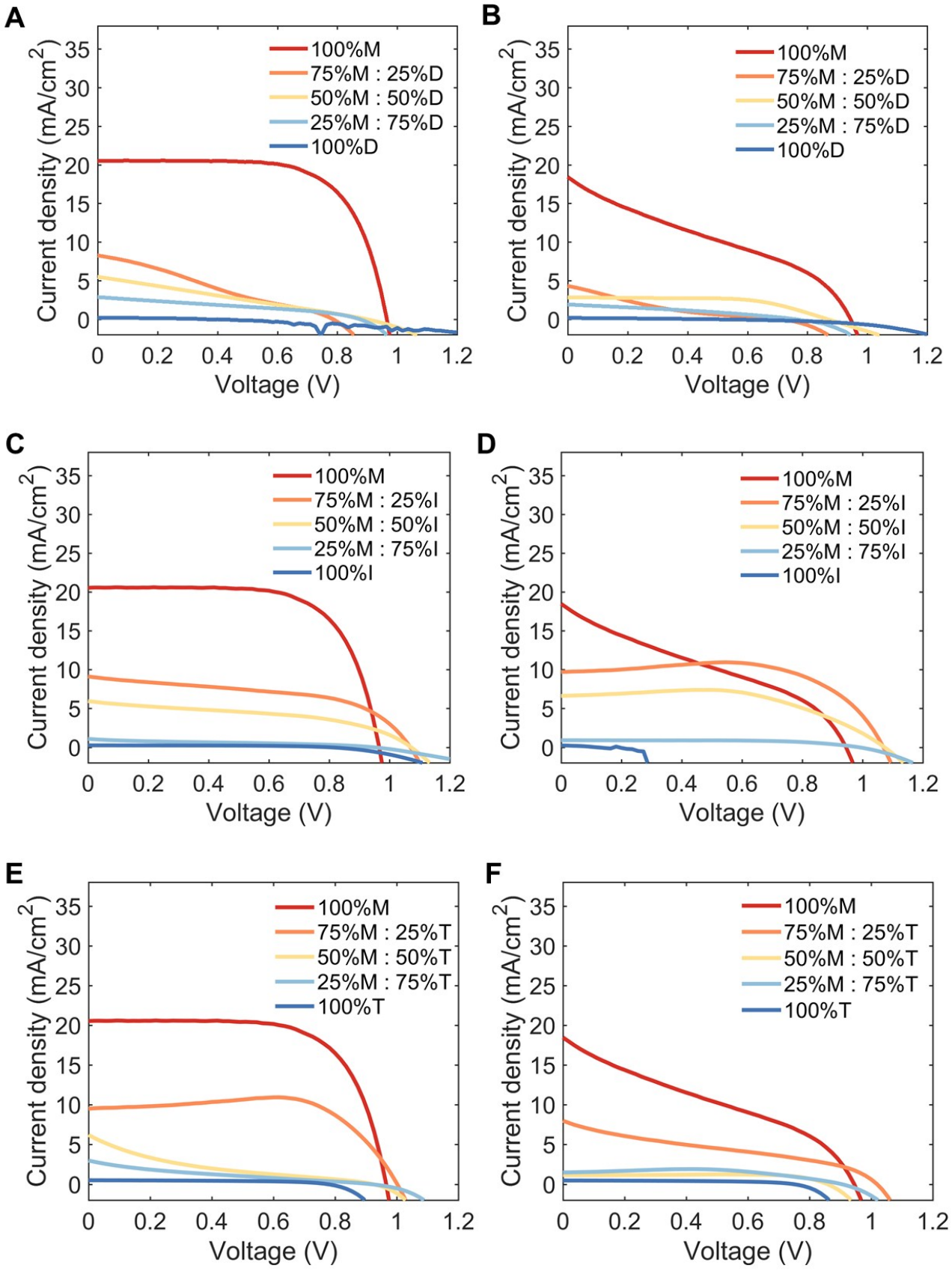
A
B
C
D
E
F
Current density (mA/cm^2)
Voltage (V)
100%M
75%M : 25%D
50%M : 50%D
25%M : 75%D
100%D
75%M : 25%I
50%M : 50%I
25%M : 75%I
100%I
75%M : 25%T
50%M : 50%T
25%M : 75%T
100%T

Table S1. The PCE, J_{SC}, V_{OC}, and FF for all the M-D, M-I, and M-T samples.

	PCE (%)			J_{SC} (mA cm^{-2})			V_{OC} (V)			FF (%)		
	25th percent-ile	75th percent-ile	Mean	25th percent-ile	75th percent-ile	Mean	25th percent-ile	75th percent-ile	Mean	25th percent-ile	75th percent-ile	Mean
M-D												
100% M	9.25	11.20	10.20	17.30	19.45	18.29	0.895	1.009	0.952	45.38	61.33	53.42
75% M: 25% D	0.30	0.95	0.68	2.43	5.92	4.25	0.595	0.690	0.647	17.60	23.45	20.83
50% M: 50% D	0.25	1.18	0.83	0.89	2.49	1.99	0.661	0.883	0.770	28.65	51.80	39.94
25% M: 75% D	0.10	0.55	0.27	0.45	2.49	1.50	0.435	0.789	0.639	24.55	23.45	20.83
100% D	0.00	0.03	0.02	0.11	0.22	0.17	0.388	0.655	0.487	28.6	34.73	31.50
M-I												
100% M	9.25	11.20	10.20	17.30	19.45	18.29	0.895	1.009	0.952	45.38	61.33	53.42
75% M: 25% I	4.75	6.60	5.70	7.69	11.15	9.33	1.013	1.070	1.037	49.43	66.93	47.41
50% M: 50% I	1.40	1.95	1.63	2.68	4.09	5.62	0.997	1.060	1.009	27.10	39.20	33.45
25% M: 75% I	0.20	0.30	0.28	0.59	0.84	0.93	0.950	0.990	0.938	32.23	44.45	40.63
100% I	0.03	0.10	0.06	0.11	0.21	0.25	0.685	0.788	0.733	44.68	56.28	49.39
M-T												
100% M	9.25	11.20	10.20	17.30	19.45	18.29	0.895	1.009	0.952	45.38	61.33	53.42
75% M: 25% T	4.00	7.25	5.33	7.68	10.16	8.72	0.942	1.019	0.970	24.30	47.88	37.83
50% M: 50% T	0.10	0.50	0.34	0.31	2.00	1.59	0.849	0.879	0.861	30.35	46.30	36.65
25% M: 75% T	0.30	0.35	0.33	1.12	2.28	1.57	0.896	0.915	0.902	18.35	27.45	22.64
100% T	0.02	0.10	0.08	0.10	0.30	0.22	0.497	0.749	0.629	44.95	57.90	51.63

Table S2. The ΔJ_{SC}^{norm} and W_{OC} for all the M-D, M-I, and M-T samples.

	ΔJ_{SC}^{norm} (1)			W_{OC} (V)		
	25th percentile	75th percentile	Mean	25th percentile	75th percentile	Mean
M-D						
100% M	0.511	0.565	0.541	0.266	0.381	0.323
75% M: 25% D	0.813	0.924	0.866	0.754	0.848	0.780
50% M: 50% D	0.922	0.972	0.938	0.564	0.791	0.683
25% M: 75% D	0.870	0.977	0.922	0.933	1.288	1.083
100% D	0.975	0.988	0.981	1.406	1.662	1.547
M-I						
100% M	0.511	0.565	0.541	0.266	0.381	0.323
75% M: 25% I	0.566	0.700	0.637	0.504	0.560	0.537
50% M: 50% I	0.582	0.801	0.696	0.840	0.903	0.891
25% M: 75% I	0.906	0.941	0.915	1.040	1.080	1.092

100% I	0.975	0.989	0.979	1.243	1.367	1.365
M-T						
100% M	0.511	0.565	0.541	0.266	0.381	0.323
75% M: 25% T	0.286	0.719	0.490	0.890	0.967	0.939
50% M: 50% T	0.824	0.973	0.859	1.095	1.126	1.113
25% M: 75% T	0.765	0.885	0.838	1.124	1.143	1.137
100% T	0.970	0.990	0.978	1.281	1.465	1.362

Figure S9. The scanning electron microscopy images for the following samples: **A.** 100% M, **B.** 75% M: 25% T, **C.** 50% M: 50% T, **D.** 25% M: 75% T, and **E.** 100% T. The scale bars are 500 nm.

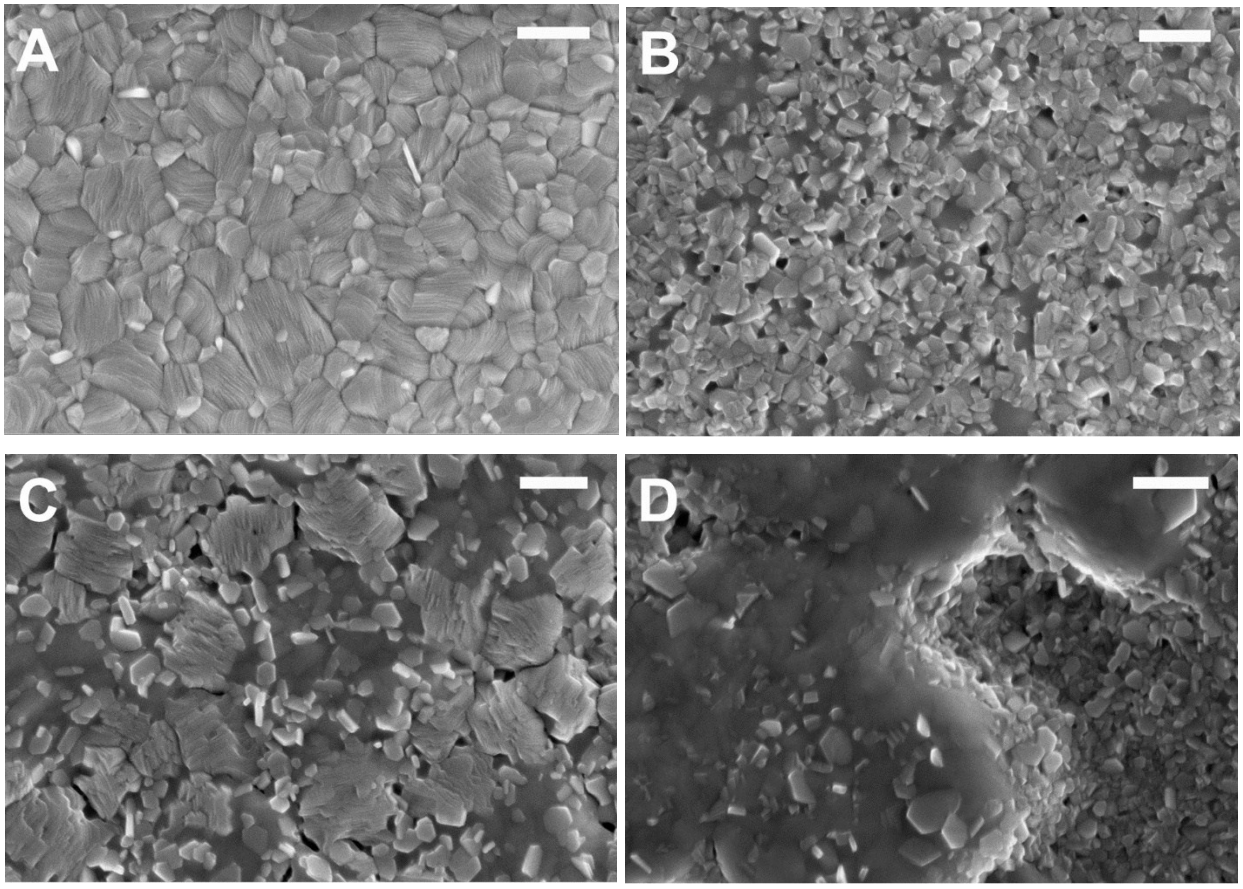

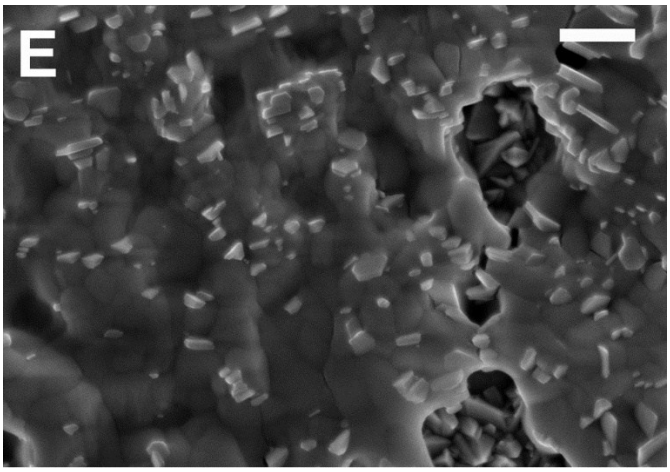

Figure S10. The W_{OC} for both phases of M-D mixtures, M-I mixtures, and M-T mixtures. Phase 1 is based on bandgap from Tauc plot fitting at 525 nm absorptance onset, and phase 2 is based on bandgap at 825 nm absorptance onset.

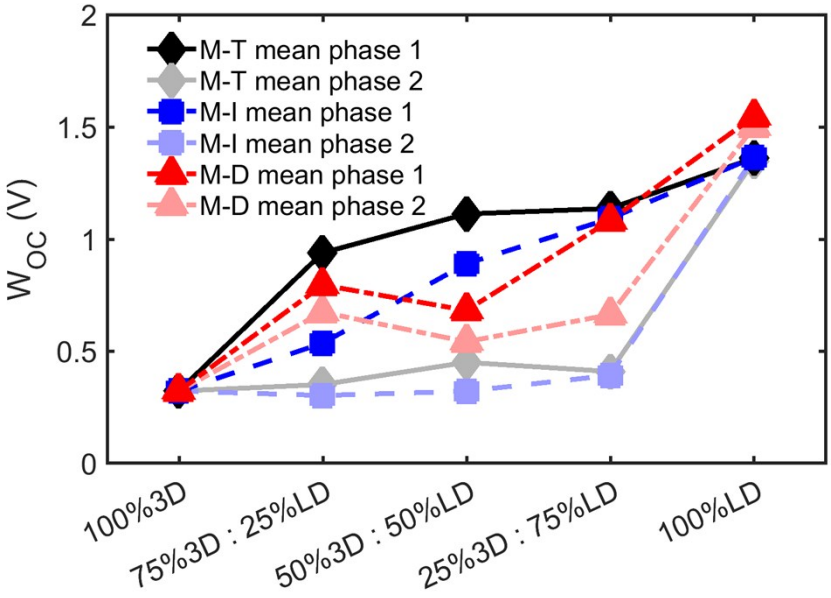

Figure S11. Change of photo-conductivity in TRMC as a function of time for **A.** 100% M **B.** 50% M: 50% T **C.** 25% M: 75% T **D.** 50% M: 50% D. All of these thin films are excited at 720 nm (excitonic peak).

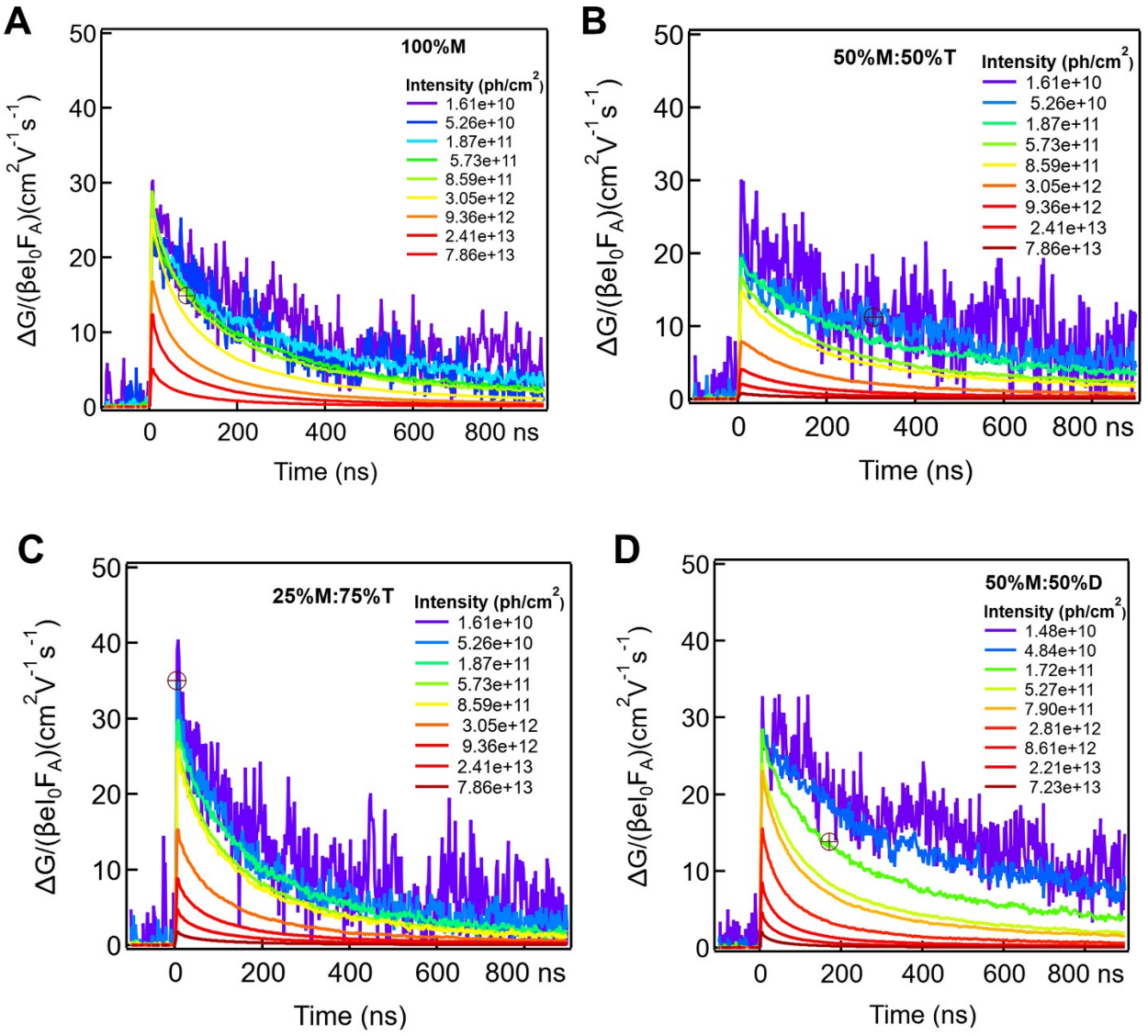

Figure S12. Change of photo-conductivity in TRMC as a function of time for **A.** 100% D **B.** 100% I **C.** 100% T. All of these thin films are excited at 490 nm (excitonic peak).

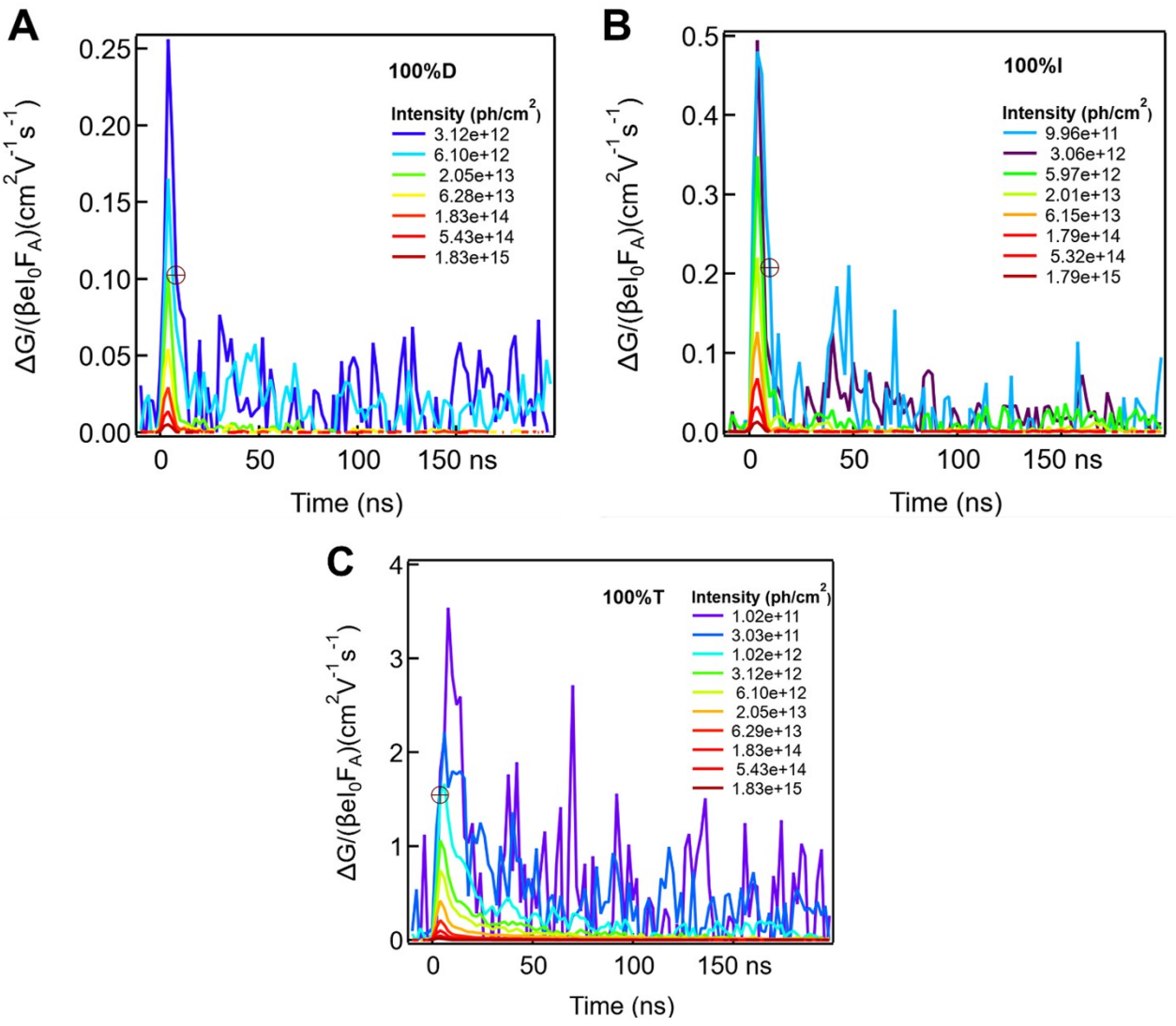

Figure S13. Half-lifetime of charge carriers based on TRMC measurement. Excited at the excitonic peaks (720 nm for 100% M, 75% M: 25% T, 50% M: 50% T, 25% M: 75% T, 50%M: 50% D, and 490 nm for 100% D, 100% T, and 100% I).

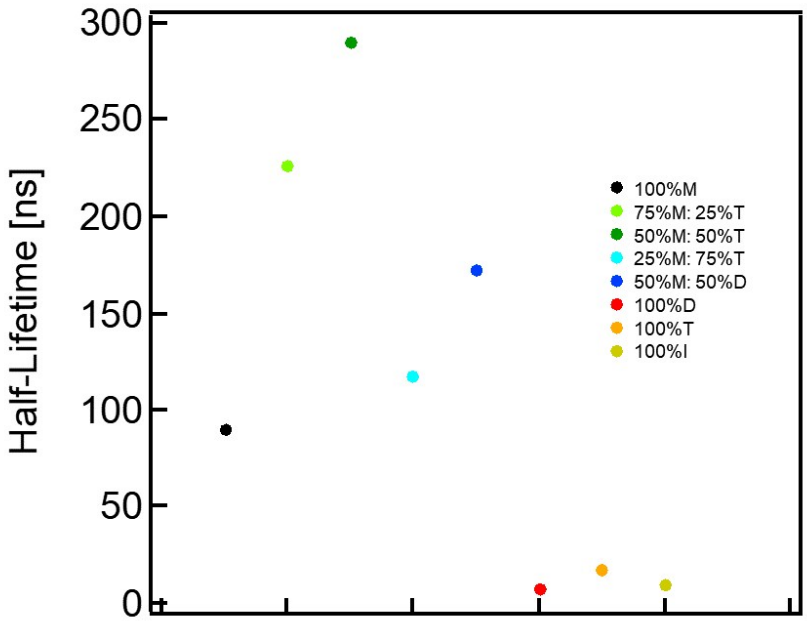

Figure S14. A. Maximum change of photo-conductivity in TRMC measurement. **B.** Half-lifetime of the charge carriers for LD perovskites, excited at 490 nm.

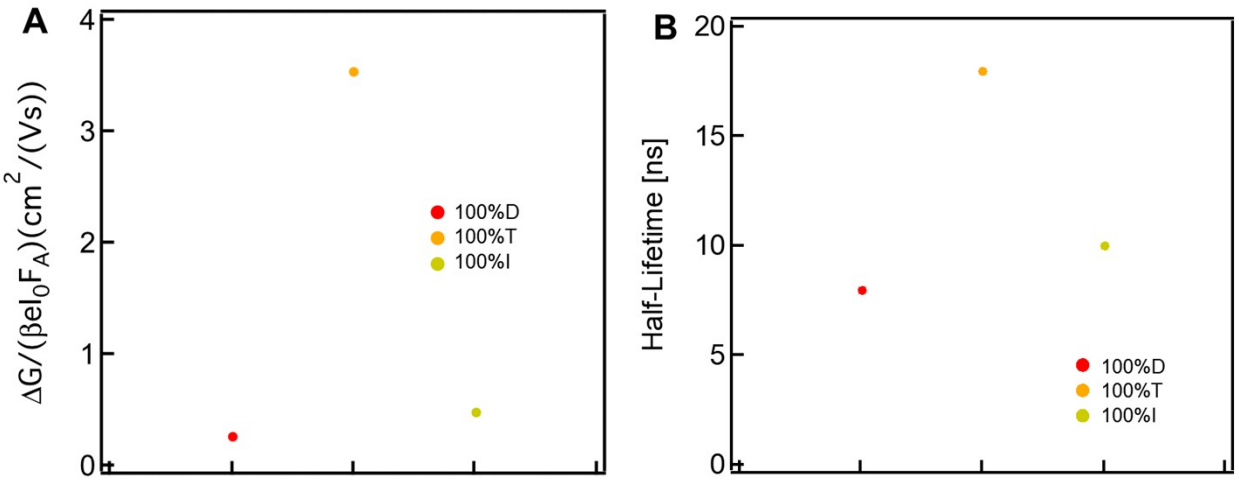

Figure S15. The absolute, average, PCE (power conversion efficiency) hysteresis, normalized for M-T, M-D, M-I alloys devices.

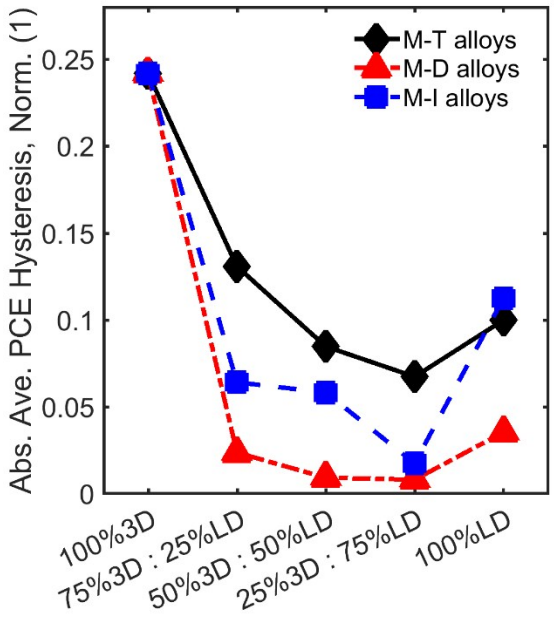

Figure S16. The change in $\Delta T/T_0$ of M-T mixtures measured using THz pump-probe method. The decay slows down with increasing T concentration up to 75% T, and then decay increases again for 100% T sample.

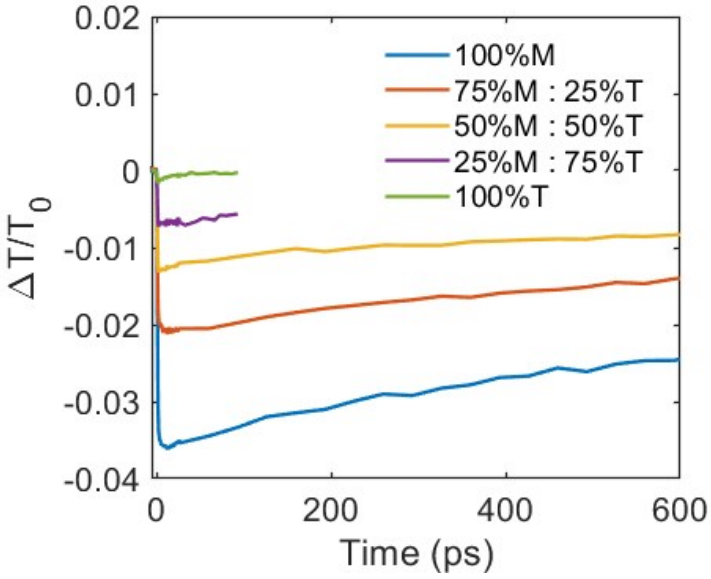

References

1. Wei F, Deng Z, Sun S, et al. The synthesis, structure and electronic properties of a lead-free hybrid inorganic–organic double perovskite $(MA)_2KBiCl_6$ (MA = methylammonium). *Mater Horizons*. 2016;3(4):328-332. doi:10.1039/C6MH00053C

2. Sun S, Fang Y, Kieslich G, White TJ, Cheetham AK. Mechanical properties of organic–inorganic halide perovskites, $CH_3NH_3PbX_3$ (X = I, Br and Cl), by nanoindentation. *J Mater Chem A*. 2015;3(36):18450-18455. doi:10.1039/C5TA03331D
3. Mancini A, Quadrelli P, Amoroso G, et al. Synthesis, structural and optical characterization of $APbX_3$ (A=methylammonium, dimethylammonium, trimethylammonium; X=I, Br, Cl) hybrid organic-inorganic materials. *J Solid State Chem*. 2016;240:55-60. doi:10.1016/j.jssc.2016.05.015